Frequency impact on the bistatic radar scattering from an ocean surface

Ahmad AWADA[1,2], Ali KHENCHAF[1] and Arnaud COATANHAY[1]
[1]ENSIETA/$E3I2$-Laboratory, 2 rue Franois Verny, Brest 29806, France
[2]INP Grenoble GIPSA-Lab/DIS, 961 rue de la Houille Blanche, BP 46, 38402 St MArtin d'Heres, France
email: {awadaah, ali.khenchaf, arnaud.coatanhay}@ensieta.fr

***Abstract*—In this paper we study the frequency impact on the normalized bistatic cross section (NBCS) of the sea surface. Numerical simulations are presented and analyzed in the frequency range going from 1 to 14 GHz (L- to K_u-band). We treat this problem with the unifying scattering model denoted small slope approximation (SSA). The computations were made by assuming the surface-height spectrum of Elfouhaily *et al* for fully developed seas. Numerical results are obtained and discussed in both forward scattering configuration and fully bistatic one for different sea states and polarization ones.**

I. Introduction

Bistatic polarimetric radars may potentially increase the available density of remote sensing radar data significantly, as relatively cheap secondary receive-only systems, operating bistatically against a single transmitter can supplement a conventional monostatic system [1]. Moreover, bistatic phenomena such as the Brewster effect can reveal target properties that are not revealed clearly in monostatic scattering.

However, radar signals frequency value represents a key parameter in remote sensing applications. The choice of this value depends on the exploring target and the geometrical configuration of the operational system. Usually, the majority of the current systems of ocean remote sensing operate in monostatic configuration and in the C-, X- and K_u-bands [2], [3] because wavelengths of these bands have the same order of the sea surface wavelengths. We can quote the ERS system operating at C-band frequency [3] and QuikSCAT system operating at K_u-band [2]. In the same way, the use of Global Positioning System (GPS) (operating at L-band) as a forwardscatter remote sensing tool has lead to fruitful research in the last few years [4].

The major publications about the sea surface works present results in each band separately. No thorough study has yet been presented in a bistatic configuration to analyze the frequency influence. This is the object of this paper. Approximate models are still a necessity owing to the insurmountable numerical complexity of realistic scattering problems [5]. We can refer to [5] which is the latest critical and up-to-date survey of the approximate models. Yet, we can quote some important models existing in the literature : the two-scale model (TSM) [6], the small slope approximation (SSA) [7], and the weighted curvature approximation WCA [8]. In this study, we choose the SSA model to treat the bistatic scattering problem. This model is a unifying theory that could reconcile small perturbation method (SPM) and Kirchhoff approximation (KA) without introducing roughness scale division parameter.

In the following section we recall briefly the SSA theoretical development and we point out the scattering dependence on the radar frequency value. The third section is devoted to NBCS numerical simulations of the ocean surface for several bistatic configuration particularly as a function of the signals frequency. The last section summarizes the paper and presents some suggestions.

II. Theoretical scattering formulation

Geometrical configuration adopted to resolve the wave-scattering problem from the sea surface is given in figure 1.

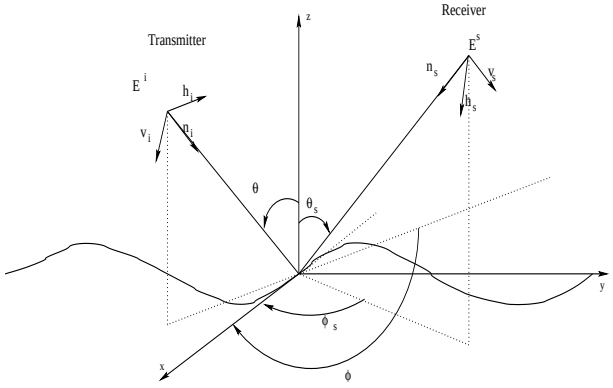

Fig. 1. Geometrical configuration for the wave-scattering from sea surface

A. The SSA model

The SSA was proposed by Voronovich [7] as a unifying theory that could reconcile SPM and KA without introducing the roughness scale division parameter K_d. It is an analytical approach, appropriate for scattering from both large- (high-frequency regime), intermediate and small-scale (low-frequency regime) roughness scales within a single theoretical scheme. Thus it encompasses both Bragg and Kirchhoff mechanisms of scattering. It can be applied to an arbitrary wavelength, provided that the tangent of grazing angles of incident/scattered angles radiation sufficiently exceeds RMS slopes of roughness. It starts from an ansatz based on the invariance properties of the Scattering Amplitude (SA). Performing a horizontal or vertical translation $\boldsymbol{d}$ affects the latter

by a phase shift $exp(-i(\boldsymbol{k}-k_0)\cdot\boldsymbol{d})$ or $exp(-i(q-q_0)\cdot\boldsymbol{d})$, so a solution is sought in the form [9] :

$$S(\boldsymbol{k},\boldsymbol{k}_0)=\int \exp[-i(\boldsymbol{k}-\boldsymbol{k}_0)\cdot\boldsymbol{r}-i(q-q_0)h(\boldsymbol{r})]\times \Phi\left[\boldsymbol{k},\boldsymbol{k}_0,\boldsymbol{r},h\right]\frac{\mathrm{d}\boldsymbol{r}}{(2\pi)^2} \quad (1)$$

where $\boldsymbol{k}_0, q_0$ are horizontal and vertical projections of the wave vector of an incident wave, and $\boldsymbol{k}, q$ are appropriate components of the wave vector of scattered wave. The unknown functional Φ is obtained by performing a functional Taylor with respect to the Fourier transform $\hat{h}$ and imposing coefficients that give consistency with SPM as $h\to 0$. In practice, only the first two orders are tractable; the higher orders become far too intricate. At first order in the slope (SSA1) we have [7] :

$$S_1(\boldsymbol{k},\boldsymbol{k}_0)=\frac{2(q\ q_0)^{1/2}}{q_k+q_0}B_1(\boldsymbol{k},\boldsymbol{k}_0)\frac{1}{(2\pi)^2}\times \int \exp[-i(\boldsymbol{k}-\boldsymbol{k}_0)\cdot\boldsymbol{r}-i(q-q_0)h(\boldsymbol{r})]d\boldsymbol{r} \quad (2)$$

To avoid the computational complexity in the second order (SSA2) and accepting an error about of 1 dB [10], we will present numerical results by using SSA at first order in the next section for different bistatic configurations.

B. Scattering dependence on the frequency value

To highlight scattering dependence on the signals frequency value, we write the scattering coefficient based on the SSA1 model for an isotropically rough surface [11] :

$$\sigma_{\alpha\alpha_0}(\boldsymbol{k},\boldsymbol{k}_0)=2\left|\frac{2q_k\ q_0}{q_k+q_0}B_{\alpha\alpha_0}(\boldsymbol{k},\boldsymbol{k}_0)\right|^2 \cdot\int_0^\infty\{e^{-\kappa[\rho(0)-\rho(r)]}-e^{-\kappa\rho(0)}\}J_0(Kr)rdr \quad (3)$$

where $\kappa=(q_k+q_0)^2$. α,α_0 corresponds to the polarization of scattered and incident plane wave respectively. To illustrate the effective parameters which can be selected under a given frequency value (for a fixed geometric condition), we plot the integrand evaluation in equation (3) for scattering configuration along the specular direction at an incident angle equal to 60° and wind speed of 4 m/s.

Figure 2 shows that the value of r over which the integrand is significant is about 2 m for L-band signals (F=1.58 GHz). Under this condition, only points on the surface less than 0.3 m apart remain correlated in their scattering contribution. For signals in Ku-band (F=14 GHz), the significant integration range of r is reduced to about 0.15 m. So, we can deduced that the effective surface parameters selected to explain scattering problem (bistatic) at K_u-band cannot be used to explain scattering at L-band.

Figure 3 points out the wind dependence on the integration range of r in L-band at an incidence of 50°. Figure 3 shows that at 7 m/s convergence of the integral along the specular direction requires integration over the lag distance about 1 m

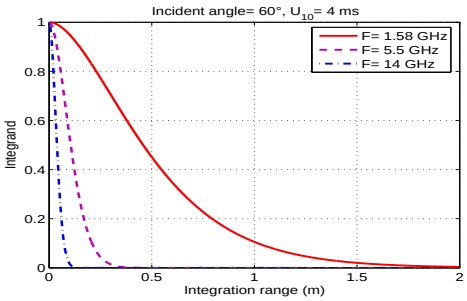

Fig. 2. Integrand evaluation of equation (3) for scattering along the specular direction for three frequencies 1.58, 5.5 and 14 GHz corresponding, respectively to L-, C- and K_u-band radar

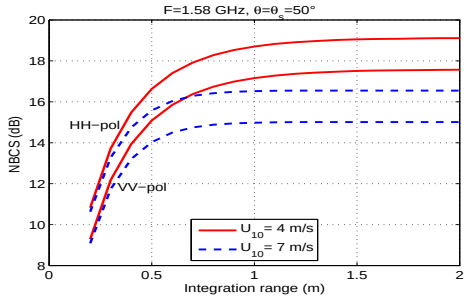

Fig. 3. Convergence of the scattering integral at 70° incidence and 1.58 GHz as a function of the lag distance for two wind speeds 4 and 7 m/s.

where the incident angle equal to 50°. For the same angle at wind speed of 4 m/s the integration range increases to about 2 m. Indeed, with increasing incident angle to 70° a large surface is needed to be integrated over, up to about 4 m at wind speed of 4m/s. It follows that only a portion of the correlation function is contributing significantly to the scattering coefficient and this portion is controlled by the frequency and how fast the correlation function decays (as a function of wind speed).

The next section is dedicated to predict the NBCS of the sea surface by using the SSA scattering model seen in section II and the Elfouhaily [12] sea surface spectrum.

III. Numerical results

In this section we present the numerical simulations to analyze the behavior of the NBCS ocean surface especially as a function of the emission frequency. Results will be presented in the case of a forward scattering configuration (along the specular direction) and in a fully bistatic configuration one. We note that a deeply comparison between the SSA and TSM model in bistatic configuration was made in [10].

A. Forward scattering : comparison between different models

The forward configuration is a particular case of the bistatic configuration where the z-axis, the incident wave vectors and the scattered wave vectors are in the same plane ($\phi=\phi_s=0^\circ$). Figure 4 compares the results yielded by the SSA with those of the geometric optic of Kirchhoff approximation (KA-GO), the small perturbation model (SPM) and the two scale

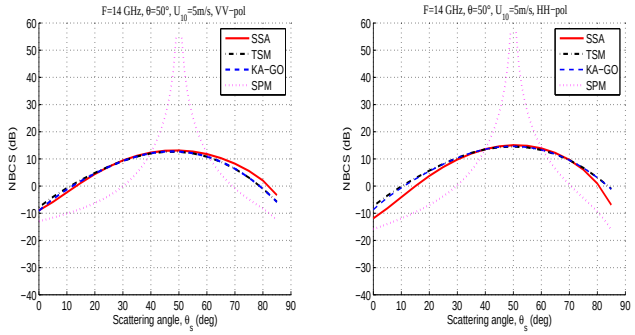

(a) Polarisation VV (b) Polarisation HH

Fig. 4. Coefficients de diffusion en fonction de l'angle d'observation en configuration propagation avant pour un angle d'incidence $\theta = 50°$, (a) Polarisation VV et (b) Polarisation HH.

model (TSM). The emitter incident angle is equal to $50°$, we vary the scattering angle from $0°$ to $85°$, electromagnetic frequency is fixed at 14 GHz (K_u-band).

As is apparent in figure 4, which is the maximum energy is received around the specular direction $50°$ which is a logical result (because this is the true specular direction as given by Snell's law). Thus, there is a good agreement between the results obtained with SSA and those of geometric optics Kirchhoff Approximation (GO-KA) near-specular directions where it is well known that the last model works well. Also, the SSA results for VV-polarization present a higher concordance with those obtained with the TSM model then for the case of HH-polarization but the difference remains within about 2 dB. Therefore, graphs in figure 4 show the limit of the SPM model in this configuration.

B. Scattering along the specular direction

This configuration involves that incident emission and reception directions must be the same and the corresponding azimuth also must be equal. we present in figure 5 the NBCS

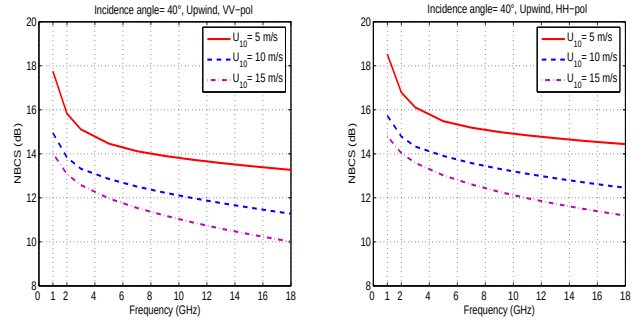

(a) VV polarization (b) HH polarization

Fig. 5. Frequency dependence on the scattering along the specular direction for $40°$ incidence angle at three wind speeds $\{5,\ 10,\ 15\text{m/s}\}$, (a) VV-polarization and (b) HH-polarization

variations along the specular direction for $40°$ incidence angle as a function of the radar frequency value for three wind speeds 5, 10 and 15 m/s for VV- and HH-polarization. As is apparent in figure 5 the NBCS values decrease with increasing of the frequency values which is the opposite behavior of the backscattering [13]. It must be noted that the difference between NRCS values at L- and K_u-band is of about 5 dB in this scattering case along the specular direction.

Figure 6 shows the NBCS variations along the specular

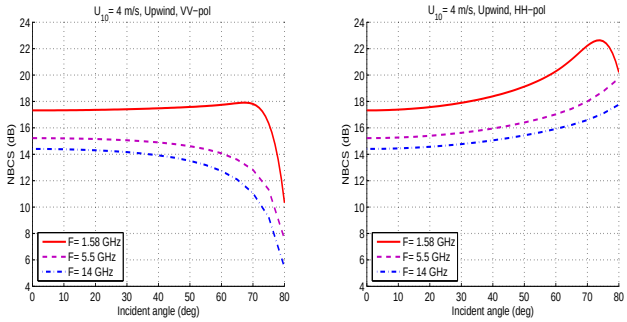

(a) VV polarization (b) HH polarization

Fig. 6. NBCS variations along the specular direction for L-, C- and K_u-band at a wind speed of U_{10}=4 m /s, (a) VV-polarization and (b) HH-polarization

direction versus the incident angle $0° - 80°$ for frequencies of 1.58, 5.5 and 14 GHz, corresponding, relatively to L-, C- and K_u-band radar. The wind speed is fixed to 4 m/s and the upwind direction is under consideration.

In examining curves in figure 6 several items of importance may be deduced. First, for both VV- and HH-polarizations the NBCS values are quasi constant in the incidence region $[0° - 60°]$. This behavior can be an important tool in exploring the sea clutter. Second, for VV-polarization in part (a) beyond $60°$ there is an important decreasing in NBCS results. on the other hand, in part (b), the horizontally polarized scattering coefficient continues to rise with incident angle up to $80°$ except for L-band frequency. Beyond $70°$, in this particular case (F= 1.58 GHz), the coefficient turns back down. This down turn is due to integration into negative correlation region [11].

C. Fully bistatic scattering dependence on the frequency

We present in figure 7 the NBCS numerical results in a fully bistatic configuration. It is defined with the following parameters: $\theta = \theta_s = 40°$, $\phi = 0$, and $\phi_s = 40°$. Both the co- and cross-polarization are simulated. In examining graphs of figure 7 we can see that contrary to the scattering along the specular direction (6), the NBCS increases with the frequency value like the backscattering case. This is due to the fact that in this geometrical configuration (fully bistatic) the Bragg mechanism of scattering becomes significant. That, as this mechanism is sensitive to capillarity waves, when the frequency increases the interaction electromagnetic signals with waves (capillarity) tends to amplify the intensity in the appropriate direction of this fully bistatic configuration.

IV. Conclusion

In this paper we have analyzed the ocean surface bistatic scattering dependence on the radar frequency value. Numerical

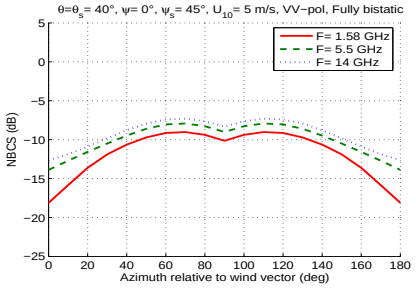

(a) VV polarization

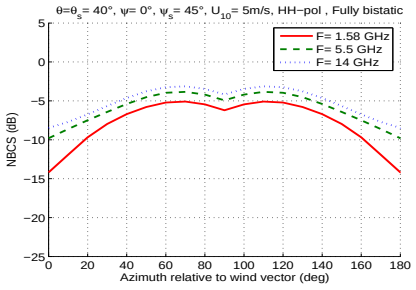

(b) HH polarization

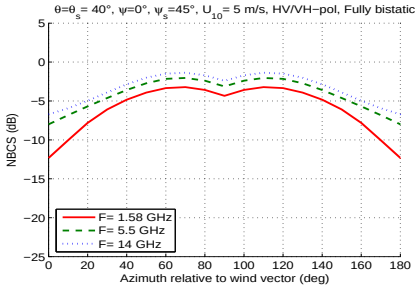

(c) VH/HV polarization

Fig. 7. NBCS variations for a fully bistatic configuration for three band frequency L, C, K_u, the incident/scattering angle is fixed to 40°, azimuth of transmitter is fixed to 0°, and azimuth of receiver equal to 45°, (a) VV-pol, (b) HH-pol, (c) VH/HV-pol

results are presented in the particular bistatic configuration (forward scattering) and in a fully bistatic one.

In the forward scattering configuration we have compared SSA results with three others models. A good similitude is obtained with the KA-GO and TSM models, the application limit of the SPM model in this configuration.

Analysis of the numerical results in the particular case of the bistatic case (the specular direction) versus the frequency value show that the NBCS decreases when the frequency increases which is an opposite behavior of the backscattering configuration. For a large scattering incident angles and at a small wind speeds, the low radar frequency (L-band) becomes unexploitable signals in the sea scattering (specular direction) which limits the using of the adopted theoretical model.

In a fully bistatic configuration, the NBCS variations versus the frequency value is the contrary of the scattering along the specular direction due to the fact of the Bragg mechanism. The recently WCA model seems to be promising to improve some particular bistatic cases predicted with the SSA model which will be exploited in our future work.

REFERENCES

[1] J. Martin-Neira, C. Mavrocordatos, and E. Colzi, "Study of a constellation of bistatic radar altimetters for mesoscale ocean applications," *IEEE trans. Geosci. Remote Sensing*, vol. 36, pp. 1898–1904, 1998.

[2] F. J. Wentz, "A model function for the ocean-normalized radar cross section at 14 GHz derived from NSCAT observations," *J. Geophys. Res.*, vol. 104, pp. 499–514, 1999.

[3] A. Bentamy, P. Queffeulou, Y. Quilfen, and K. Katsaros, "Ocean surface wind fields estimated from satellite active and passive microwave instruments," *IEEE trans. Geosci. Remote Sensing*, vol. 37, pp. 2469–86, 1999.

[4] V. U. Zavorotny and A. V. Voronovich, "Scattering of GPS signals from the ocean with wind remote sensing application," *IEEE trans. Geosci. Remote Sensing*, vol. 38, no. 2, pp. 951–964, 2000.

[5] T. Elfouhaily and C. A. Guérin, "A critical survey of approximate scattering wave theories from random rough surfaces," *Waves Random Media*, vol. 14, pp. R1–R40, 2004.

[6] A. Khenchaf, "Bistatic scattering and depolarization by randomly rough surfaces: application to the natural rough surfaces in X-band," *Waves Random Media*, vol. 11, pp. 61–89, 2001.

[7] A. G. Voronovich, "Small-slope approximation for electromagnetic wave scattering at a rough interface of two dielectric half-spaces," *Waves Random Media*, vol. 4, pp. 337–367, 1994.

[8] T. Elfouhaily, S. Guignard, R. Awadallah, and D. R. Thompson, "Local and non-local curvature approximation: a new asymptotic theory for wave scattering," *Waves Random Media*, vol. 13, pp. 321–328, 2003.

[9] A. G. Voronovich and V. U. Zavorotny, "Theoretical model for scattering of radar signals in k_u- and c-bands from a rough sea surface with breaking waves," *Waves Random Media*, vol. 11, pp. 247–269, 2001.

[10] A. Awada, M. Y. Ayari, A. Khenchaf, and A. Coatanhay, "Bistatic scattering from an anisotropic sea surface: Numerical comparison between the first-order SSA and the TSM models," *Waves in Random and Complex Media*, vol. 16, no. 3, pp. 383–394, 2006.

[11] A. Awada, A. Khenchaf, and A. Coatanhay, "Bistatic radar from an ocean surface at L-band," *in the proceedings of the IEEE Radar Conference*, Verona, NY, USA 2006.

[12] T. Elfouhaily, B. Chapron, K. Katsaros, and D. Vandemark, "A unified directional spectrum for long and short wind-driven waves," *J. Geophys. Res.*, vol. 102, no. C7, pp. 781–796, 1997.

[13] A. K. Fung and K. K. Lee, "A semi-empirical sea-spectrum model for scattering coefficient estimation," *IEEE Jou. Ocean. Engine.*, vol. 7, no. 4, pp. 166–176, 1982.